

## Asymmetries in Above-Threshold Ionization

M. Bashkansky,<sup>(a)</sup> P. H. Bucksbaum, and D. W. Schumacher

*AT&T Bell Laboratories, Murray Hill, New Jersey 07974*

(Received 29 March 1988)

Above-threshold atomic photoemission by intense elliptically polarized light is not symmetric with respect to reflection about either principal polarization axis, contrary to predictions. Simultaneous reflection about both axes is symmetric. These asymmetries occur in helium, krypton, and xenon photoelectron spectra, and depend on the laser intensity and polarization, and the electron energy. Possible mechanisms are discussed.

PACS numbers: 32.80.Rm, 42.50.Hz

Since the discovery of above-threshold ionization (ATI) in 1979,<sup>1</sup> ATI experiments have uncovered many interesting and unusual phenomena related to the non-linear interactions between intense radiation and atoms. Among these are the scattering of free electrons by light,<sup>2</sup> suppression of threshold photoionization in intense fields,<sup>3</sup> suppression of low-energy photoelectrons for circularly polarized light,<sup>4</sup> and, of course, the absorption of excess photons, which is ATI itself. Here we report yet another new phenomenon: The violation of fourfold symmetry in the distribution of ATI photoelectrons generated by elliptically polarized light. This new effect not only is unexpected, but is in opposition to existing ATI theories.

ATI produced by elliptically polarized light has been investigated before.<sup>5</sup> The current studies were motivated by a previous experiment which showed that angular distributions with elliptically polarized light resemble the predictions of an approximate nonperturbative theory proposed by Keldysh,<sup>6</sup> and revised and extended by Faisal<sup>7</sup> and by Reiss<sup>8</sup> (the KFR approximation). In the preceding work, electrons were collected over one quadrant in the azimuthal ( $\phi$ ) plane perpendicular to the laser direction  $\mathbf{k}$ , spanning angles between the polarization semimajor and semiminor axes. The polarization was retarded by  $\xi = 80^\circ$ , where the retardation  $\xi$  is implicitly defined by the equation for the unit vector along the instantaneous electric field,

$$\hat{\mathbf{e}} = \hat{\mathbf{x}} \cos(\xi/2) \cos(kz - \omega t) + \hat{\mathbf{y}} \sin(\xi/2) \sin(kz - \omega t).$$

(The helicity  $h$  is related to  $\xi$  by  $h = \sin\xi$ ). If the electromagnetic interaction is restricted to electric dipole transitions, it is easily shown in perturbation theory that the final-state electron distribution must be symmetric with respect to reflection about  $\hat{\mathbf{x}}$  and  $\hat{\mathbf{y}}$ , the major and minor polarization axes, and also must be invariant under  $\xi \rightarrow -\xi$  ( $h \rightarrow -h$ ). In that case, the distribution may be represented by a function of the form

$$\sum_{n=-\infty}^{\infty} a_n \cos 2n\phi, \quad (1)$$

where  $\phi$  is the azimuthal angle (with respect to  $\hat{\mathbf{x}}$  in the

$x$ - $y$  plane). Fits of the data by this function<sup>5</sup> were found to match closely the predictions of the KFR model, which also contains this symmetry.

Recent improvements in the laser and the optics have enabled us to extend these measurements to the full azimuthal plane. We find that expression (1) is generally inadequate to fit the data, but must be expanded to

$$\sum_{n=-\infty}^{\infty} (a_n \cos 2n\phi + b_n \sin 2n\phi). \quad (2)$$

This is the most general angular distribution consistent with invariance under rotation about  $\mathbf{k}$  ( $z$  axis) by  $\pi$ . The light-atom system must be invariant with respect to this rotation in order to satisfy spatial isotropy.

The current data were obtained with an amplified mode-locked Nd-doped yttrium aluminum garnet laser and its second harmonic. The pulse width was variable between 0.10 and 0.15 nsec, and was monitored by standard autocorrelation techniques. The spatial profile of the beam was a truncated central Airy disk, focused to an area 20  $\mu\text{m}$  in diameter at half intensity. The focus was measured with a simple achromatic microscope imaged onto a television camera. Ionization occurred in a magnetically and electrically shielded vacuum with a base pressure of  $1 \times 10^{-9}$  Torr, seeded with  $10^8$  to  $10^{11}$  atoms/cm<sup>3</sup> of xenon, krypton, or helium.

Electrons were collected by two methods. The first was a time-of-flight spectrometer subtending a solid angle of 0.003 sr in the polarization plane. In this device, angular distributions were obtained by rotation of the polarization, which was set as follows: First, the laser light passed through a linear polarizer, then through a half-wave plate, a quarter-wave plate, and a second half-wave plate. The retardation plates were all crystal-line quartz, multiple order, antireflection coated, and commercially supplied. Although only one half-wave and one quarter-wave plate are required to fix any polarization, the additional half-wave plate provides more control. Here the first half-wave plate may be moved while the quarter-wave plate remains fixed, to establish the helicity without movement of the orientation of the major and minor polarization axes. The second half-

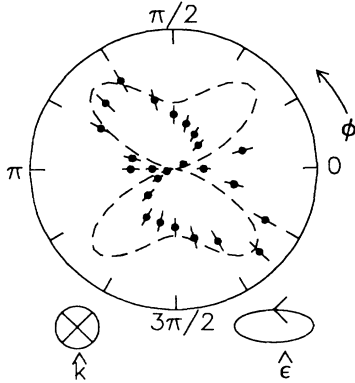


FIG. 1. Azimuthal angular distribution for nineteen-photon ionization of krypton by 1064-nm light of 150-psec duration, focused to approximately  $2 \times 10^{13}$  W/cm<sup>2</sup>, and elliptically polarized with helicity  $h = -0.82$ . Dashed line is prediction of the KFR theory, with no ponderomotive effects included. Data fail to display fourfold symmetry predicted by this and other ATI theories.

wave plate then rotates the polarization ellipse to the desired orientation. The scheme is imperfect, because wave plates are seldom manufactured to the required tolerance, and are also extremely sensitive to alignment in the mount. To combat these problems, the polarization was analyzed at each orientation. We were thus able to maintain the retardation and orientation to within  $\pm 2^\circ$ . The *sign* of the helicity (i.e., right- versus left-handed polarization) was determined by a zero-order circular analyzer, constructed with stretched polyethylene film and a linear polarizer.<sup>9</sup>

A different detector was employed to obtain higher angular resolution, at the expense of energy resolution, or to view angles away from the polarization plane. This second device consisted of a set of retarding grids, followed by microchannel electron multipliers subtending 0.08 sr ( $66^\circ$  opening angle), centered in the polarization plane perpendicular to  $\mathbf{k}$ . Electrons from the channel plates impinged onto a phosphor-coated glass plate, which was viewed from behind by a television camera. Electrons were collected over many laser pulses, resulting in two-dimensional histograms in  $\theta$  (the polar angle with respect to  $\mathbf{k}$ ) and  $\phi$  (the azimuthal angle). By rotation of the polarization to different orientations, a mosaic was constructed consisting of the full angular distribution between  $\theta = 60^\circ$  and  $\theta = 120^\circ$ , over all angles in  $\phi$ .

Data from both detectors are in startling disagreement with the expected fourfold azimuthal symmetry. A typical example is shown in Fig. 1, which displays the full angular distribution of the ATI electrons from krypton ionized by nineteen 1064-nm photons. In this example, the laser was "right elliptically polarized" (*negative* helicity), with  $h = -0.82$  ( $\xi = -55^\circ$ ). The dashed line is the KFR prediction, with neglect of all ponderomotive effects. The obvious discrepancy is the strong asymmetry with respect to reflection about either the major or

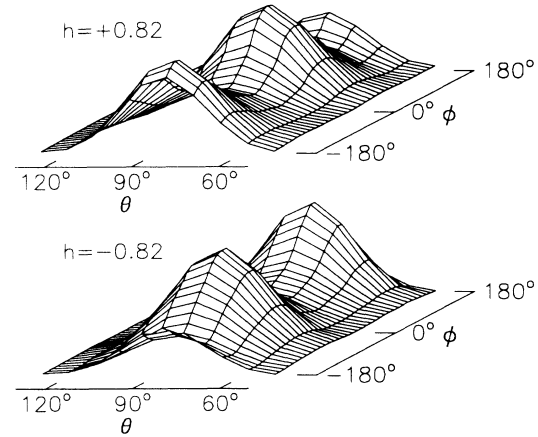


FIG. 2. Angular distributions in the azimuthal ( $\phi$ ) and polar ( $\theta$ ) directions, for xenon photoionized by 1064-nm light with helicity  $h = +0.82$  (top) and  $h = -0.82$  (bottom). Data set contains all ATI peaks with energies of 9 eV and higher, summed together. The laser wave vector  $\mathbf{k}$  lies along  $\theta = 0$ . This view emphasizes the fore-aft symmetry about the polarization plane defined by  $\theta = \pi/2$ . The only observed asymmetry is in the azimuthal direction.

minor axes. Simultaneous reflection  $\hat{\mathbf{x}} \rightarrow -\hat{\mathbf{x}}$ ,  $\hat{\mathbf{y}} \rightarrow -\hat{\mathbf{y}}$  is symmetric, as expected [see expression (2) above].

We have investigated the dependence of the asymmetry on the ATI peak, the atom, the laser wavelength and intensity, the sign and magnitude of the retardation, and the laser focus parameters. We have also investigated the polar-angle dependence and find that electrons are nearly all emitted in the polarization plane, symmetric with respect to the forward and backward hemispheres (Fig. 2). The only unexpected asymmetry is in the azimuthal angles.

The asymmetry is nearly always present for elliptical polarization, but has never been observed for either linear or circular polarization. (For circular polarization, such an asymmetry is forbidden by spatial isotropy.) In addition, the asymmetric angular distributions reverse with a reversal of the sign of the laser helicity. This is shown for several different cases in Fig. 3. This reversal is required by parity invariance. Along with symmetry under  $\hat{\mathbf{x}} \rightarrow -\hat{\mathbf{x}}$ ,  $\hat{\mathbf{y}} \rightarrow -\hat{\mathbf{y}}$ , these features provide important tests to rule out a large class of potential experimental systematic errors, such as stray magnetic fields. The lines in Figs. 3 and 4 are fits by Fourier series of the form in expression (2).

As the absolute value of the helicity increases, starting from  $h = 0$  (linear polarization), the asymmetries gradually appear. This can be seen in the series of distributions for krypton in Fig. 4. This figure also shows the gradual change in the distributions with the ATI peak, and a change with laser intensity. The latter is somewhat obscured by the well-known ponderomotive scattering effects which tend to smear out the angular distribu-

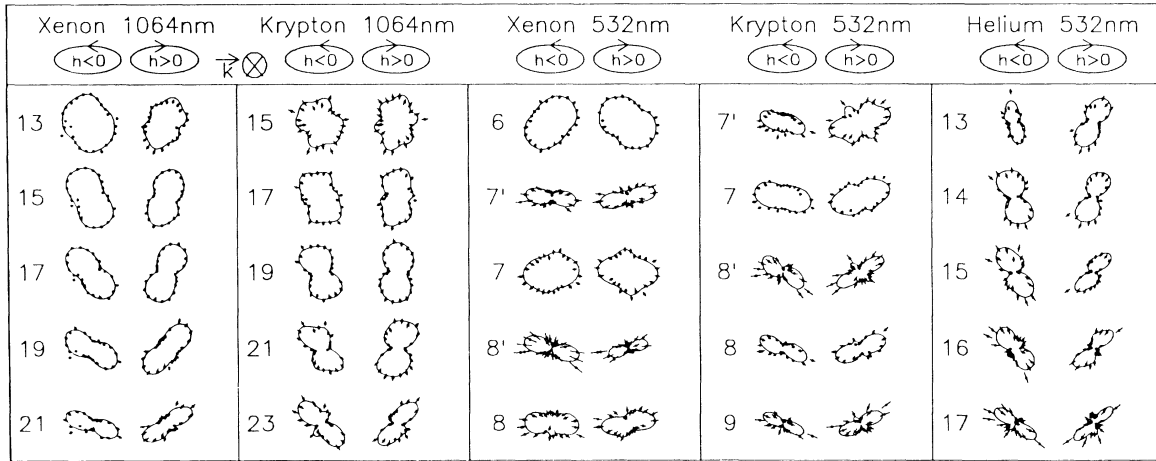


FIG. 3. Comparison between data obtained with positive-helicity light ( $h = +0.82$ ), and data obtained under the same conditions but with the helicity reversed ( $h = -0.82$ ). The laser pulse width was 0.10 to 0.12 nsec. Xe 1064 nm:  $I_{\text{peak}} = 4 \times 10^{13}$  W/cm<sup>2</sup>;  $P_{1/2}$  and  $P_{3/2}$  final states were not resolved, so numbers indicate photons absorbed for the  $P_{3/2}$  final state. Kr 1064 nm:  $I_{\text{peak}} = 4 \times 10^{13}$  W/cm<sup>2</sup>;  $P_{3/2}$  final states only. Xe 532 nm:  $I_{\text{peak}} = 1 \times 10^{13}$  W/cm<sup>2</sup>; primed numbers designate photons absorbed to the final  $P_{1/2}$  state; unprimed numbers designate the  $P_{3/2}$  state. Kr 532 nm:  $I_{\text{peak}} = 1.5 \times 10^{13}$  W/cm<sup>2</sup>; primes mean the same as for Xe 532 nm. Helium 532 nm:  $I_{\text{peak}} = 1 \times 10^{14}$  W/cm<sup>2</sup>.

tions for slower electrons at high intensities.<sup>10</sup>

We have considered many possible explanations for the asymmetry. Experimental artifacts have been virtually ruled out. However, the KFR approximation forbids an asymmetry of this form. Likewise, multiple-order

perturbation theory also forbids this, so long as all single-photon virtual transition amplitudes are electric dipole. Possible breakdowns of these approximations include higher multipole effects, atomic-structure effects such as intermediate resonances, and ponderomotive scattering produced by the laser focus.

Atomic-structure effects are suggested in at least one instance, where the asymmetries reverse for six-photon 532-nm ionization of xenon to the  $P_{3/2}$  ion final state (Fig. 3). Possible contributions from ponderomotive scattering have been examined through direct experiments, simulations, and calculations, and we currently believe that they play no role in these asymmetries.

Although we lack a theory for this new intense-field phenomenon, there is a semiclassical argument that provides a qualitative explanation. An electron that ionizes by absorbing many elliptically polarized photons carries off several units of angular momentum. In helium, for example, where the initial atom and final ion are both  $s$  states, the electron carries off about  $nh\hbar$  units of angular momentum, where  $h$  is the light helicity and  $n$  is the number of photons absorbed. If we neglect spin-flip transitions, the electron-ion system must therefore have an impact parameter  $b$  of

$$b \approx nh\hbar / [2m_e(n\hbar\omega + E_G - U_P)]^{1/2}. \quad (3)$$

Here  $E_G$  is the (negative) ground-state energy, and  $U_P$  is the ponderomotive potential energy of the electron, which subtracts from its drift kinetic energy.<sup>11</sup> The quantum mechanical manifestation of the classical impact parameter is the exclusion of the final-state wave function from the ion by a centrifugal potential barrier.

During the escape of the electron from the ion field,

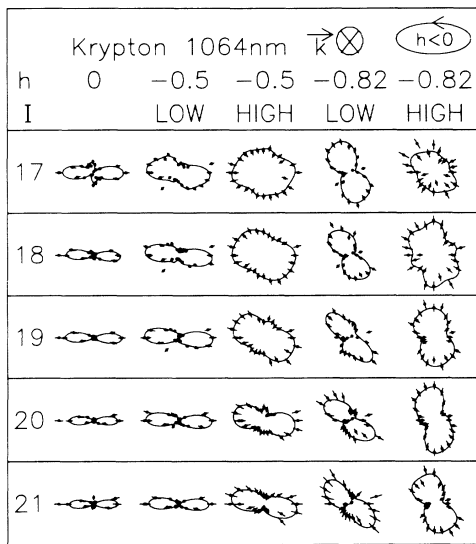


FIG. 4. Azimuthal distributions for various retardations and laser intensities, for krypton photoionized by 1064-nm light. Numbers to the left of each row designate photons absorbed to the  $P_{3/2}$  ion final state for each ATI peak. First column: linear polarization,  $I_{\text{peak}} = 2.5 \times 10^{13}$  W/cm<sup>2</sup>. Second column:  $h = -0.5$ ,  $I_{\text{peak}} = 2 \times 10^{13}$  W/cm<sup>2</sup>. Third column:  $h = -0.5$ ,  $I_{\text{peak}} = 4 \times 10^{13}$  W/cm<sup>2</sup>. Fourth column:  $h = -0.82$ ,  $I_{\text{peak}} = 2 \times 10^{13}$  W/cm<sup>2</sup>. Fifth column:  $h = -0.82$ ,  $I_{\text{peak}} = 4 \times 10^{13}$  W/cm<sup>2</sup>.

the angular momentum is constant (if we neglect further interactions with the laser field), but linear momentum is not. For a Coulomb potential, a classical electron describes a hyperbolic trajectory. The asymptotic momentum deviates from the momentum at the point of closest approach by an angle given by

$$\Phi_{\text{dev}} = \frac{\hbar}{|\hbar|} \sin^{-1} \left[ \left( 1 + \frac{2(n\hbar\hbar)^2(n\hbar\omega + E_G - U_P)}{m_e e^4} \right)^{-1/2} \right]. \quad (4)$$

For example, consider negative-helicity 532-nm light, retarded to  $\xi = -55^\circ$  ( $h = -0.82$ ), incident on helium (shown in Fig. 3). Electrons ejected after absorbing fourteen photons have an energy of approximately 8 eV, and for the peak intensity in Fig. 3, approximately 2.5 eV of this total is in the form of ponderomotive potential energy. These numbers imply an angular deviation, during the electrons' transit out of the ion potential, of  $-8^\circ$ , i.e., *counterclockwise* when viewed along  $+\hat{z}$ . The helium spectra for  $h = -0.82$  in Fig. 3 do appear to be distorted counterclockwise from the distributions predicted by the KFR theory. These classical ideas do not explain all of the observations, but they may suggest a physical principle responsible for the broken symmetry.

We gratefully acknowledge spirited discussion with M. Mittleman, and comments by T. J. McIlrath, who suggested that we study helium.

<sup>(a)</sup>Present affiliation: Physics Department, Columbia University, New York, NY 10027.

<sup>1</sup>P. Agostini, F. Fabre, G. Mainfray, G. Petite, and N. Rahman, Phys. Rev. Lett. **42**, 1127 (1979).

<sup>2</sup>P. H. Bucksbaum, M. Bashkansky, and T. J. McIlrath, Phys. Rev. Lett. **58**, 349 (1987).

<sup>3</sup>P. Kruit, J. Kimman, H. G. Muller, and J. J. van der Wiel, Phys. Rev. A **28**, 248 (1983).

<sup>4</sup>P. H. Bucksbaum, M. Bashkansky, R. R. Freeman, T. J. McIlrath, and L. F. DiMauro, Phys. Rev. Lett. **56**, 2590 (1986).

<sup>5</sup>M. Bashkansky, P. H. Bucksbaum, and D. W. Schumacher, Phys. Rev. Lett. **59**, 274 (1987).

<sup>6</sup>L. V. Keldysh, Zh. Eksp. Teor. Fiz. **47**, 1945 (1964) [Sov. Phys. JETP **20**, 1307 (1965)].

<sup>7</sup>F. H. M. Faisal, J. Phys. B **6**, L89 (1973).

<sup>8</sup>H. R. Reiss, Phys. Rev. A **22**, 1786 (1980).

<sup>9</sup>This procedure is described in F. S. Crawford, *Waves*, (McGraw-Hill, New York, 1967).

<sup>10</sup>R. R. Freeman, T. J. McIlrath, P. H. Bucksbaum, and M. Bashkansky, Phys. Rev. Lett. **57**, 3156 (1986).

<sup>11</sup>The ponderomotive potential of an electron in an intense laser field is discussed by T. J. McIlrath, P. H. Bucksbaum, R. R. Freeman, and M. Bashkansky, Phys. Rev. A **35**, 4611 (1987).